Virus Research 260 (2019) 151–162

Contents lists available at ScienceDirect

Virus Research

journal homepage: www.elsevier.com/locate/virusres

Classification of fetal resilience to porcine reproductive and respiratory syndrome (PRRS) based on temporal viral load in late gestation maternal tissues and fetuses

Carolina M. Malgarin[a], Roman Nosach[a], Predrag Novakovic[a], Muhammad Suleman[a], Andrea Ladinig[b], Susan E. Detmer[a], Daniel J. MacPhee[a], John C.S. Harding[a,*]

[a] Western College of Veterinary Medicine, University of Saskatchewan, S7N 5B4, Canada
[b] University of Veterinary Medicine, 1210, Vienna, Austria

ARTICLE INFO

Keywords:
Swine
Virus
Transmission
Resistance
Random forest
Intrauterine growth retardation

ABSTRACT

Although porcine reproductive and respiratory syndrome virus (PRRSV) readily crosses the maternal fetal interface (MFI) in third trimester, fetal resilience varies within litters. The aim of this study was to characterize PRRSV-2 concentration in MFI and fetuses at five time points after experimental inoculation of late gestation gilts and use this information to classify potentially resistant, resilient and susceptible fetuses. The secondary objective was to verify the relationship between PRRS viral load and intrauterine growth retardation (IUGR). Three PRRSV-inoculated pregnant gilts and 1 sham-inoculated control were euthanized at five time points in days post infection (DPI; 2, 5, 8, 12, 14). The preservation status of each fetus was determined and MFI samples adjacent to the umbilical stump of each fetus, as well as serum, thymus, umbilical cord and amniotic fluid were collected. Viral load was quantified using probe-based reverse-transcriptase quantitative PCR (RT-qPCR) targeting PRRSV NVSL 97-7895 ORF7. Our result show the MFI was largely PRRSV infected by 2 DPI and virus was first detected in fetal sera and umbilical cord by 5 DPI, and in fetal thymus and amniotic fluid by 8 DPI. This indicates that PRRSV-2 quickly crossed the placenta and traveled toward the fetus via umbilical circulation within one week of the dam's inoculation. Fetal compromise was first observed on 8 DPI and increased progressively through to 14 DPI. However, several factors were associated with fetal resilience. The random forest model identified that 'viral load in fetal thymus' and duration of infection ('DPI') as the most important factors predicting fetal resilience and resistance. Moreover, IUGR fetuses had lower viral load and were less frequently compromised or dead compared to non-IUGR and average cohorts. Understanding the mechanisms of fetal resilience to PRRSV will improve selection strategies for replacement gilts.

1. Introduction

Porcine reproductive and respiratory syndrome virus 2 (PRRSV) belongs to the order *Nidovirales*, family *Arteriviridae*, genus *Porartevirus* and causes a disease with worldwide distribution that affects pigs of all ages (Zimmerman et al., 2012). Besides the well-studied respiratory disease, PRRSV can also cause reproductive losses associated with fetal death, abortions and birth of weak piglets (Terpstra et al., 1991; Zimmerman et al., 2012) making PRRS one of the costliest swine diseases in North America with approximately 45% of annual losses associated with the reproductive disease (Holtkamp et al., 2013).

PRRSV replication in the maternal-fetal interface (MFI) is biologically important for the outcome of reproductive PRRS since it is positively related to viral RNA concentration in the fetal serum and thymus (, b; Ladinig et al., 2015b and also one of the determinants of fetal preservation status (Ladinig et al., 2015a). How and when the virus

Abbreviations: AMN, amniotic fluid; CPE, cytopathic effects; CTRL, control group/gilts; DEC, decomposed fetus; DNQ, detected not quantified (viral RNA detected in sample but the amount was below the threshold required for quantification, typically $< 10^2$ or 10^3 per mg or μL); DPI, days post inoculation; END, endometrium; IUGR, intra-uterine growth retardation; MEC, meconium stained fetus; MFI, maternal-fetal interface; PLC, placenta; PRRSV, porcine reproductive and respiratory syndrome virus; RT-qPCR, reverse transcriptase quantitative polymerase chain reaction; SER, serum; THY, thymus; VIA, viable fetus; VL, viral load/concentration

* Corresponding author at: 52 Campus Dr., Saskatoon, Saskatchewan, S7N 5B4, Canada.
E-mail addresses: carolina.malgarin@usask.ca (C.M. Malgarin), rvn767@mail.usask.ca (R. Nosach), predrag.novakovic@usask.ca (P. Novakovic), dr.suleman.muhammad@gmail.com (M. Suleman), andrea.ladinig@vetmeduni.ac.at (A. Ladinig), susan.detmer@usask.ca (S.E. Detmer), d.macphee@usask.ca (D.J. MacPhee), john.harding@usask.ca (J.C.S. Harding).

https://doi.org/10.1016/j.virusres.2018.12.002
Received 3 October 2018; Received in revised form 30 November 2018; Accepted 4 December 2018
Available online 05 December 2018

crosses the MFI is not completely understood, but it is known that Sn^+CD163^+ macrophages are the target cells for PRRSV replication in the MFI (Karniychuk et al., 2013; Karniychuk and Nauwynck, 2009; Novakovic et al., 2017; Van Gorp et al., 2008; Whitworth and Prather, 2017). Three hypotheses for the possible routes of transmission of the virus from endometrium (END) to placenta (PLC) have been proposed by Lager and Mengeling (Lager and Mengeling, 1995) and reviewed by Karniychuk and Nauwynck (Karniychuk and Nauwynck, 2013): 1) a cell-to-cell transmission with virus transiting through infected END macrophages to END epithelium to fetal trophoblastic epithelium to PLC macrophages; 2) as free viral particles through or between END epithelium and trophoblast epithelial cells; and 3) as infected macrophage-associated virus migration from END to PLC.

After transmission to fetuses, the virus replicates in fetal tissues with thymus (THY) reported as the primary site of viral replication (Rowland, 2010). Our research group has previously shown that the severity of PRRS can be highly variable within individual litters, and PRRSV RNA concentration in fetal thymus, serum (SER), PLC and END differs across preservation category (Ladinig et al., 2014b). Fetal meconium-staining of the skin, a condition associated with fetal stress in which the fetus is covered in fecal material, is an early clinical indicator of PRRSV-induced fetal compromise and is associated with the presence of fetal lesions (Novakovic et al., 2018, 2016) and severity of apoptosis in the MFI (Novakovic et al., 2017). Meconium staining varies in severity and distribution in infected litters (Ladinig et al., 2014b) as does fetal susceptibility and resistance to the virus (Ladinig et al., 2014b). Fetal infection is a strong predictor of fetal compromise and death (Ladinig et al., 2015a) and viral replication within fetuses and clustering within litters appear to be important in the pathogenesis of reproductive PRRS because fetal infection and death increases the probability of adjacent fetuses becoming PRRSV-infected or dying (Ladinig et al., 2015a). A previous study determined that intrauterine growth retarded (IUGR) fetuses have lower PRRS viral load (VL) in THY and adjacent MFI than non-IUGR and larger fetuses when collected at 21 days post inoculation (DPI) (Ladinig et al., 2014a), potentially indicating a mechanism of fetal resilience.

Understanding the sequential movement of PRRSV across all reproductive and fetal tissues is important to more fully understand disease progression, further characterize the effects of IUGR on VL, as well as identify potential mechanisms of fetal resistance and resilience. The current study aimed to: a) characterize by RT-qPCR the temporal movement of PRRSV across the MFI and into fetal tissues within two weeks of maternal inoculation in late gestation; b) determine when the first signs of fetal compromise occur; c) develop an algorithm to classify and/or identify resistant, resilient and susceptible fetuses; and d) confirm the relationship between fetal resistance/resilience to IUGR to understand how this condition potentially impacts transmission and susceptibility.

2. Materials and methods

2.1. PRRSV propagation

A virulent PRRSV-2 (formerly type 2) strain (NVSL 97-7895 ; GenBank Accession No. AF325691) was propagated for an experimental challenge by infecting PRRSV susceptible MARC-145 cells as previously described (Ge et al., 2016; Suleman et al., 2018). The culture conditions were set at 37 °C under 5% CO_2 and maintained in Modified Eagle Medium (MEM) supplemented with 7% heat-inactivated fetal bovine serum, 0.25 μg/ml fungizone, 100 U/ml penicillin, and 10 μg/ml streptomycin. Cytopathic effects (CPE) were observed at 24, 48 and 72 h post infection. The infected culture was frozen at −80 °C after 72 h with > 70–75% CPE and viral titration was conducted using MARC-145 for calculating tissue culture infective dose 50 ($TCID_{50}$) as previously described (Suleman et al., 2011).

2.2. Animals

Twenty purebred Landrace gilts were purchased from a high health, PRRSV-free farm rearing pigs using husbandry and vaccination protocols compliant with the National Farm Animal Care Council 2014 Code of Practice (http://www.nfacc.ca/pdfs/codes/pig_code_of_practice.pdf) and the Canadian Pork Excellence Program (http://www.cpc-ccp.com/canadian-pork-excellence). Six months old gilts were selected, puberty stimulated, estrus synchronized and inseminated with Yorkshire semen using single sire matings. At ~80 days of gestation, gilts were transferred to biocontainment level 2 animal care facilities at the University of Saskatchewan. After five days of acclimation, blood was collected via jugular venipuncture, and 15 gilts blocked by sire were inoculated (INOC) with 4 mL of 1×10^5 $TCID_{50}$ of NVSL 97-7895 ; 2 mL intramuscularly and 1 mL into each nostril. Five gilts housed in a separate room were similarly mock inoculated with minimum essential medium (CTRL).

2.3. Experimental procedures

One CTRL and three INOC gilts were humanely euthanized and sampled at each of five different DPI (2, 5, 8, 12, and 14). On the day of sample collection, the dams and litters were collected one at a time, starting with the CTRL gilt, with the aim of completing all fetuses within 45 min of death to maintain mRNA quality. Gilts were euthanized by intravenous administration of pentobarbital sodium (Euthanyl Forte®, Bimeda-MTC Animal Health Inc., Canada) followed by cranial-captive bolt shot, pithing, and exsanguination. Blood was collected from each gilt in plain, anti-coagulant free tubes. The abdominal cavity was opened by a ventral midline incision, the reproductive lymph node collected, and the gravid reproductive tract removed and placed in a trough where maternal blood was washed from the external surface.

2.3.1. Fetal preservation and sample collection

The uterine horns were opened from ovarian tip (right and left) to the uterine body along the anti-mesometrial border. The fetuses were numbered sequentially in each horn, starting from the one closest to each ovary; R1 for the right side and L1 for the left, and progressing to the body of the uterus. An umbilical clamp was placed on each fetal cord to prevent cross-contamination and loss of fetal blood.

The preservation status of each fetus was categorized as viable (VIA = live, normal skin color), meconium-stained (MEC = live, normal skin covered with meconium) and decomposed (DEC = dead, pale skin, sometimes edematous). Meconium staining was further characterized by severity based on the distribution of meconium; either on the face only (MEC-F), or face and body (MEC-B) (Supplemental file 1). Mummified fetuses (dehydrated, dark brown color, crown-rump length < 20 cm) were not sampled because they were deemed to have died due to other reasons prior to the time of inoculation.

Fetuses were placed on individual trays, weighed and crown-to-rump length measured. Following dissection, the brain and liver were also weighed individually to assess the degree of IUGR based on the brain:liver ratio (with greater brain:liver indicative of IUGR; a.k.a. “brain sparing”). Fetal blood from the axillary artery, amniotic fluid (AMN) from stomach, and THY were collected from each fetus. Blood was refrigerated until serum separation. Serum and AMN were frozen and stored at −80 °C, whereas THY was snap frozen in liquid nitrogen.

A 3 × 3 cm section of uterus adjacent to the umbilical stump was collected, washed of blood, and placed (PLC side up) in a plastic weigh boat on ice for 10 min. The PLC was manually separated from the END with forceps and multiple 0.5 to 1.0 cm pieces of both tissues were stored at −80 °C. An approximately 3 cm section of the umbilical cord of each fetus was cut 2 to 5 cm from the placental attachment and similarly stored.

2.4. Quantification of PRRSV RNA

PRRSV RNA extraction and RT-qPCR reaction were performed as previously described (Ladinig et al., 2014b). Briefly, viral RNA was extracted using commercial kits (RNeasy MiniKit, Qiagen, Toronto, Canada) and a QIAcube extraction robot (Qiagen) from 30 mg of tissue sample after homogenization using lysis buffer (Qiagen RLT buffer plus beta-mercaptoethanol) and steel microspheres. Extraction of SER and AMN was performed manually using 140 µL of sample and the Qiamp Viral RNA kit (Qiagen). For each procedure, a known positive control and an extraction negative control were run simultaneously.

Specific primers, previously designed for the PRRSV strain NVSL 97-7895 (Ladinig et al., 2014b) were used: PRRS-2 F - 5′- TAATGGGCTG GCATTCCT -3′, PRRS-1R - 5′-ACACGGTCGCCCTAATTG -3′, probe PRRS-P1 - 5′ HEX-TGTGGTGAATGGCACTGATTGRCA-BHQ2 3′. The plasmid HindIII pCR2.1TOPO-NVSL containing a 446 bp sequence of ORF-7 was used for the standard curve (five points: 10^7, 10^5, 10^3, 10^2, 10^1 run in triplicate on each plate). Each RT-qPCR reaction consisted of BioRad iTaq Universal Probes 1-Step Kit (10 µL/reaction), water (8 µL/reaction), forward and reverse primers (0.5 µL/reaction), probe (0.5 µL/reaction), and reverse transcriptase enzyme (BioRad) (0.5 µL/reaction). For each 96 well plate, 35 samples were run in duplicate, along with three extraction negative controls, a positive control, and a RT-qPCR NTC. The RT-qPCR reaction consisted of reverse transcription for 30 min at 50 °C for cDNA synthesis, followed by a PCR initial activation step of 10 min at 95 °C, 40 cycles of denaturation for 30 s at 95 °C, and annealing/extension for 30 s at 59 °C. SPC charts were used to monitor the variability of the positive controls in each run. If the Ct standard deviation between the duplicates was higher than 1.5 or if one of the two duplicates had a negative Ct, the samples were re-analyzed. Incongruent negative results (e.g. a negative fetal SER result with a positive THY result) were repeated to confirm negativity. Results were reported as $\log_{10}$ target RNA concentration per mg of tissue or µL of SER/AMN. Heat maps were created to visualize changes in VL by fetus across tissues and DPI.

2.5. Classification of resistant, resilient and susceptible fetuses

Fetal resistance, resilience and susceptibility to PRRSV infection were determined using previous definitions as guidelines (Bishop and Woolliams, 2014; Ladinig et al., 2014b; Richardson, 2016). As an initial step, the average PRRSV RNA concentration in fetal PLC, UMB, SER, THY, AMN was calculated and plotted against fetal preservation score (0 = VIA, 1 = MEC-F, 2 = MEC-B, 3 = DEC) (X-axis) for all fetuses from inoculated gilts. Breakpoints of 1.5 for fetal preservation score and 3.5 $\log_{10}$ copies/mg or µL for average VL were used to distinguish four quadrants representing fetal resistance, resilience, susceptibility or ultra-susceptibility in the bottom-left, top-left, top-right, and bottom-right quadrants, respectively. A classification approach was then used to determine which variables were most important in predicting fetal resistance, resilience and susceptibility. Random Forest classifier models (Machado et al., 2015) (RandomForestClassifier from sklearn.ensemble) were constructed in a Jupyter notebook and plotted using a confusion matrix (confusion_matrix from sklearn.metrics). The data (205 inoculated fetuses from all DPI) was split into training and test datasets in a 70:30 ratio (train_test_split from sklearn.cross_validation). A full model of 100 trees (100 permutations) was created by including potential predictor variables of fetal resistance, resilience and susceptibility: DPI, sex, categorized brain:liver ratio (−1 = Z score < 1 SD from the mean; +1 = Z score > 1 SD from the mean; 0 = Z score between −1 and +1 SD), and VL in sera and each fetal tissue (dichotomized according to natural break points in the data: 0 = < 4 $\log_{10}$ copies/mg or µL; 1 = > 4 $\log_{10}$ copies/mg or µL). Given that fetal preservation score was initially used to classify fetal resistance, resilience and susceptibility, it was not included in the full model. Although average VL in tissues and sera was also used to initially classify fetuses, the full model included each individual tissue separately with the goal of identifying the most important tissue(s) for classification. Precision, recall and F1 scores, and the relative importance of each variable were determined. Variables with the lowest relative importance value were removed in a backward stepwise manner until the most parsimonious model with greatest precision, recall and F1 scores was obtained.

2.6. Data analysis

Descriptive and statistical analyses were performed using Stata 14 (Stata-Corp, College Station, TX). Fetal IUGR was categorized using the brain:liver weight ratio at each DPI (separately for inoculated and CTRL litters), where fetuses with brain:liver one or more standard deviation below and above the mean were classified as non-IUGR and IUGR, respectively. Fetuses with brain:liver between -1 and +1 SD were considered average (AVG). Kruskal-Wallis with post hoc Dunn tests were performed to assess significant differences in VL in all the tissues amongst the three IUGR groups for each DPI. A Sidak test was used to adjust P value to account for multiple comparisons. Differences in the frequency of compromised (MEC and DEC) versus VIA fetuses across IUGR groups were evaluated using an Exact test. For all analyses, $P < 0.05$ was considered statistically significant *a priori*.

3. Results

Five of the 15 inoculated gilts had a decreased appetite for one or two days, but no other clinical signs related to PRRSV-infection were observed. PRRSV RNA was not detected in any gilt sera prior to inoculation or in any CTRL gilt sera, fetal sera or tissue. Inoculated gilts were viremic from 2 to 14 DPI, having the viral concentration peak at 5 DPI (Fig. 1). The study included 276 fetuses in total with 205 from inoculated gilts. The litter size was 13.8 in average. In control gilts, 70/71 (98.6%) fetuses were VIA and 1/71 (1.4%) was MEC. In inoculated gilts, 158/205 (77.1%) fetuses were VIA, 37/205 (18%) were MEC-F, 3/205 (1.5%) were MEC-B, and 7/205 (3.4%) were DEC.

3.1. PRSSV transmission across maternal and fetal tissues by day post inoculation

Heat maps (Fig. 2A–E) were developed to visually assess the

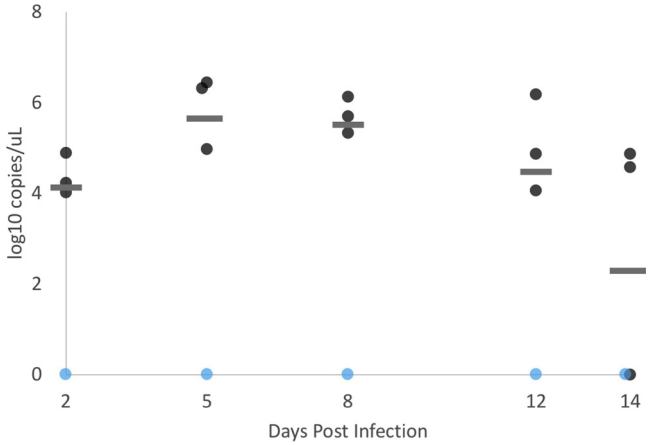

Fig. 1. Median serum PRRSV RNA concentration in gilt sera. PRRSV RNA concentration ($\log_{10}$/µL sera) in inoculated gilts between 2 and 14 days post inoculation (DPI) quantified using a probe-based RT-qPCR specific for NVSL 97-7895. Horizontal bars represents the median value of three gilts. Control gilts are represented in light blue and inoculated gilts in dark grey. Different gilts are represented each day. All gilts were positive at 2 DPI. Peak levels were noted on 5 DPI which gradually decrease over 14 DPI. Viral RNA in sera at 0 DPI and from all control gilts were negative. Overlapping data points have been "jiggled" for visual representation.

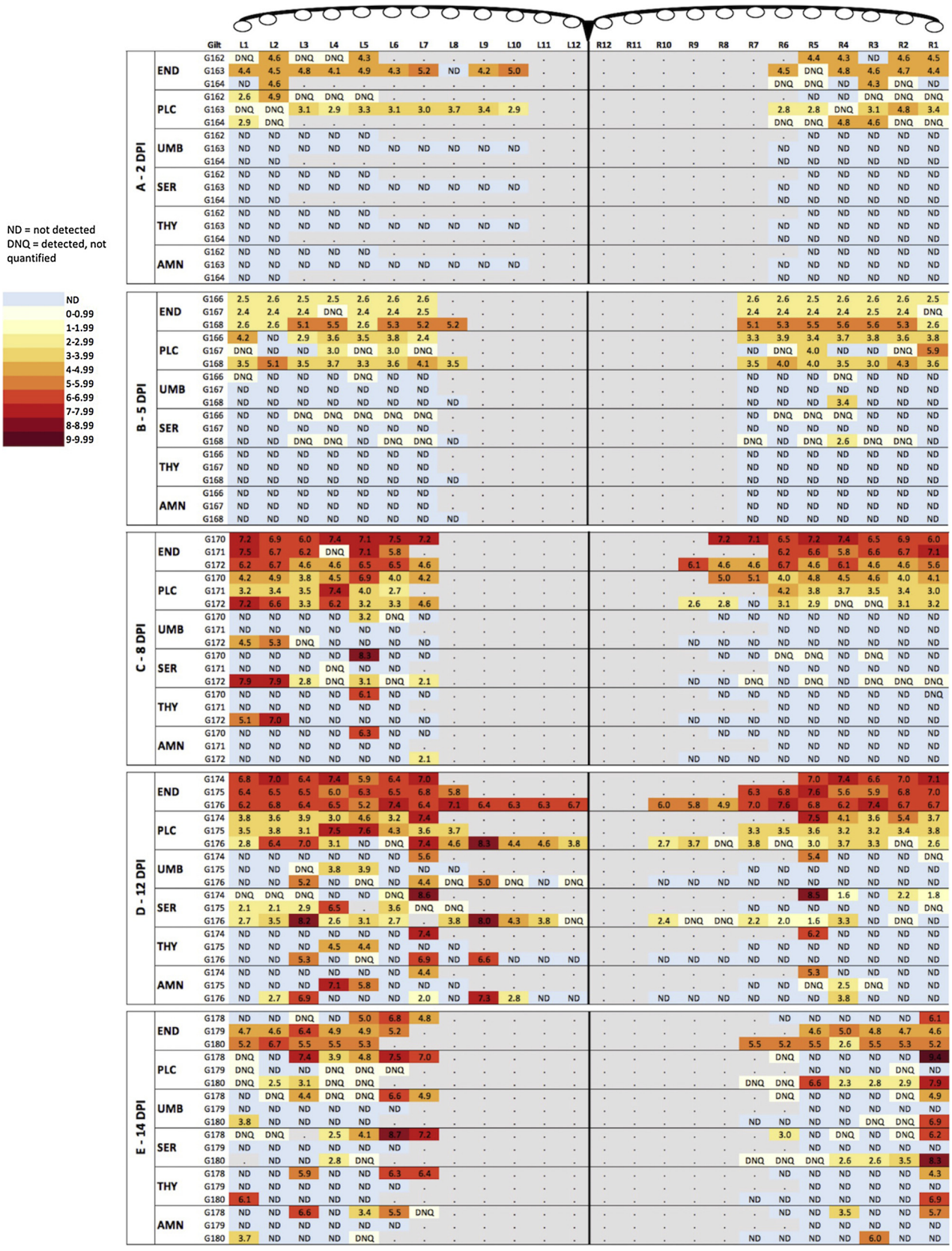

Fig. 2. Viral load heat maps by tissue and fetal preservation. Individual cells represent the PRRSV RNA concentration (log_{10} copies per mg or μL) in various maternal and fetal samples. Five blocks (A–E) each represent a different day post-inoculation (DPI) from 2 to 14. Fetal location within the left (L) and right (R) uterine horns is specified along the header (L1-L12, R1-R12). Each row represents a litter with gilt identity listed in the left column. Viral load is indicated numerically in each cell and by cell color, with light blue signifying "non-detected" (ND), pale yellow signifying "detected, not quantified" (DNQ), and quantifiable samples represented on a color gradient from light yellow (for lowest concentration) to dark red (highest concentration). Color intensity increases from top to bottom coinciding with greater viral load in more tissues at higher DPI. END = endometrium, PLC = placenta, UMB = umbilical cord, SER = fetal sera, THY = fetal thymus, AMN = amniotic fluid.

Table 1
Descriptive summary of fetal infection rates and viral load in tissues by days post inoculation.

	2 DPI	5 DPI	8 DPI	12 DPI	14 DPI
Endometrium					
Number (%) positive fetuses/total	29/34 (85)	43/43 (100)	43/43 (100)	49/49 (100)	28/36 (78)
Mean (SE) viral load	3.8 (0.1)	3.2 (0.2)	6.2 (0.2)	6.6 (0.1)	3.9 (0.1)
Median (IQR) viral load	4.4 (0.4)	2.5 (2.7)	6.5 (1.2)	6.5 (0.7)	5.2 (0.7)
Placenta					
Number (%) positive fetuses/total	32/34 (94)	37/43 (86)	42/43 (98)	48/49 (98)	21/36 (58)
Mean (SE) viral load	2.8 (0.1)	3.0 (0.1)	4.0 (0.2)	4.0 (0.2)	2.1 (0.6)
Median (IQR) viral load	2.8 (0.6)	3.5 (0.8)	3.9 (1.4)	3.7 (1.3)	2.8 (4.9)
Umbilical cord					
Number (%) positive fetuses/total	0	4/43 (9)	5/43 (12)	13/49 (26)	13/36 (36)
Mean (SE) viral load	–	1.8 (0.5)	3.2 (0.8)	3.2 (0.5)	3.5 (0.5)
Median (IQR) viral load	–	1.5 (1.1)	3.2 (3.0)	3.8 (3.8)	2.3 (2.7)
Serum					
Number (%) positive fetuses/total	0	17/43 (39)	17/43 (39)	36/49 (73)	19/36 (53)
Mean (SE) viral load	–	1.9 (0.1)	3.0 (0.6)	3.1 (0.4)	3.5 (0.5)
Median (IQR) viral load	–	1.9 (0.5)	1.8 (1.1)	2.2 (1.7)	2.6 (2.4)
Thymus					
Number (%) positive fetuses/total	0	0	4/43 (9)	8/49 (16)	6/36 (17)
Mean (SE) viral load	–	–	5.1 (1.0)	5.5 (0.6)	6.0 (0.4)
Median (IQR) viral load	–	–	5.6 (2.8)	5.7 (2.3)	6.2 (0.6)
Amniotic fluid					
Number (%) positive fetuses/total	0	0	2/43 (5)	13/49 (26)	9/36 (25)
Mean (SE) viral load	–	–	4.2 (2.1)	4.1 (0.6)	4.2 (0.6)
Median (IQR) viral load	–	–	4.2 (4.2)	3.7 (3.3)	3.7 (2.3)

DPI = days post inoculation, SE = standard error, IQR = interquartile range. The prevalence of infection increases across DPI (left to right). Viral load in fetal tissues decreases proportionally as distance from endometrium increased (top to bottom).

concentration of PRRSV RNA detected in maternal and fetal samples at each DPI and to identify temporal patterns in infection. On each, the identity of each gilt was listed in the left column and the fetal position in the uterine horn along the top row with the PRRSV RNA concentration (log_{10}/mg or μL) of each fetus presented in corresponding cells arranged in sections for each tissue. Cells were coloured on a scale from light yellow (low VL) to dark red (high VL). Descriptive statistics including number of RNA positive fetuses, median and mean VL are presented in Table 1 by tissue and DPI. Trends across DPI are discussed below. Supplemental files 2 to 7 show PRRSV RNA concentration in fetuses, similar to Fig. 2, except using heat maps organized by tissue, rather than DPI.

The preservation status of individual fetuses (VIA, MEC-F, MEC-B, DEC) by DPI was temporally assessed (Fig. 3A) with fetal PRRS severity represented along a light to dark grey color scale. The mean PRRSV RNA concentration increased in all tissues as fetal preservation progressed stepwise from VIA to MEC-F, MEC-B and finally to DEC (Fig. 3B).

3.1.1. Two days post-inoculation (Fig. 2A, Fig. 3)

The END and PLC were promptly infected after inoculation. PRRSV RNA was detected in either END, PLC or both tissues of all 2 DPI fetuses indicating an efficient mechanism(s) for maternofetal transmission. Quantifiable levels of virus were detected in the majority of fetuses in END (22/34; 65%) and PLC (18/34; 52%) with VL typically in the 3–4 log_{10}/mg range (lower end of quantifiable range) indicating viral replication was well established in these tissues. No PRRSV RNA was detected in UMB, SER, THY and AMN indicating the PLC is the initial site of PRRSV replication. All the fetuses were VIA.

3.1.2. Five days post-inoculation (Fig. 2B, Fig. 3)

The first evidence of PRRSV infection in UMB and SER was at 5 DPI. PRRSV RNA was detected in 4/43 (9%) of UMB and 17/43 (40%) of SER samples, most at DNQ levels. All 43 fetuses were VIA and all fetal THY and AMN samples remained negative at 5 DPI. The fetuses of one gilt (G167) had notably lower levels (prevalence and concentration) of viral RNA in PLC compared to the two other 5 DPI litters and no evidence of PRRSV infection in any fetal tissue, possibly suggesting a greater level of gilt-level resistance and/or resilience.

3.1.3. Eight days post-inoculation (Fig. 2C, Fig. 3)

At 8 DPI, the first compromised fetuses were observed as well as the evidence of PRRSV infection of THY and AMN. Five fetuses in the uterine locations of one litter (G170) showed facial meconium staining; four with no or low VL in fetal tissues and SER, and one with high VL in SER, THY and AMN. The latter fetus (G170-L5) was pale in appearance in addition to being meconium stained. There was a single DEC fetus (G171-R1) that had blood-tinged, sticky exudate on its face, distinctly different from meconium staining.

PRRSV RNA was detected in all END samples and 42/43 PLC samples. The prevalence of infection was greater in SER (17/43; 40%) than in THY (4/43; 9%) or AMN (2/43; 4.5%). The highest VL was observed in the pale fetus. Five other fetuses with quantifiable levels of virus in fetal tissues were in a single litter suggesting greater litter-level susceptibility. PRRSV RNA was not detected in the DEC fetus. Whether or not this death was a consequence of PRRSV infection is unknown.

3.1.4. Twelve days post-inoculation (Fig. 2D, Fig. 3)

Forty-one percent (20/49) of fetuses were compromised, compared to under 14% (6/43) at 8 DPI. Four fetuses were DEC; two in each of two litters. Sixteen fetuses were MEC (16/49, 33%); all confined to face. Ten of 20 compromised fetuses were in a single litter suggesting greater litter-level susceptibility. PRRSV RNA was detected in the SER of all except one MEC fetus but was only sporadically detected in fetal tissues (UMB, THY, AMN). However, PRRSV RNA was detected in the fetal tissues of numerous VIA fetuses in seemingly random locations, and typically in more than one tissue of each fetus. The exception was three fetuses in one litter (G175-R3/4/5) in which PRRSV RNA was detected in AMN but not in UMB, SER or THY. This pattern is suggestive of interfetal transmission from an index (R4) fetus to its neighbours R3 and R5. The greatest PRRSV RNA detection frequency was in SER (36/47; 77%).

3.1.5. Fourteen days post-inoculation (Fig. 2E, Fig. 3)

Clinical signs were more severe than at 12 DPI with fifty-eight percent of fetuses (21/36) showing compromise, including the first evidence of severe levels of meconium staining on face and/or body of

A)

DPI	gilt	L1	L2	L3	L4	L5	L6	L7	L8	L9	L10	L11	L12	R12	R11	R10	R9	R8	R7	R6	R5	R4	R3	R2	R1	% compromised
2 DPI	G162	V	V	V	V	V	.	.	.	.	.	.	.	.	.	.	.	.	.	.	V	V	V	V	V	0%
	G163	V	V	V	V	V	V	V	V	V	V	.	.	.	.	.	.	.	.	V	V	V	V	V	V	0%
	G164	V	V	.	.	.	.	.	.	.	.	.	.	.	.	.	.	.	.	V	V	V	V	V	V	0%
5 DPI	G166	V	V	V	V	V	V	V	.	.	.	.	.	.	.	.	.	.	V	V	V	V	V	V	V	0%
	G167	V	V	V	V	V	V	V	.	.	.	.	.	.	.	.	.	.	V	V	V	V	V	V	V	0%
	G168	V	V	V	V	V	V	V	V	.	.	.	.	.	.	.	.	.	V	V	V	V	V	V	V	0%
8 DPI	G170	V	V	V	F	F	V	V	.	.	.	.	.	.	.	.	.	F	F	V	V	V	F	V	V	33%
	G171	V	V	V	V	V	V	.	.	.	.	.	.	.	.	.	.	.	.	V	V	V	V	V	D	8%
	G172	V	V	V	V	V	V	V	.	.	.	.	.	.	.	.	V	V	V	V	V	V	V	V	V	0%
12 DPI	G174	V	V	V	V	F	F	F	.	.	.	.	.	.	.	.	.	.	.	.	F	F	V	V	V	42%
	G175	V	V	V	D	D	V	V	V	.	.	.	.		.	.	.	.	V	V	V	V	V	V	V	13%
	G176	V	F	D	F	F	F	D	F	F	V	F	V	.	.	F	V	F	V	V	F	V	V	V	F	62%
14 DPI	G178	V	F	D	F	V	B	F	.	.	.	.	.	.	.	.	.	.	.	F	F	V	F	F	F	77%
	G179	B	V	V	F	V	V	.	.	.	.	.	.	.	.	.	.	.	.	.	V	V	V	V	V	18%
	G180	D	F	V	F	F	.	.	.	.	.	.	.	.	.	.	.	.	F	F	F	F	V	V	B	75%

B)

Fetal Preservation Score	n	PRRSV RNA concentration (log10 copies per mg or µL) END	PLC	UMB	SER	THY	AMN
VIA	158	3.4 (2.7)	2.2 (1.9)	0.2 (0.7)	0.6 (1.4)	0.1 (0.8)	0.2 (0.8)
MEC-FACE	37	5.2 (2.5)	3.6 (2.6)	1.1(1.9)	2.7 (2.6)	1.1 (2.3)	1.0 (2.1)
MEC-BODY	3	5.5 (1.1)	5.1 (4.4)	4.5 (3.9)	5.7 (4.9)	4.4 (3.8)	1.8 (3.2)
DEC	7	5.9 (1.0)	5.7 (3.0)	3.7 (1.7)	4.9 (4.3)	4.7 (2.3)	4.6 (2.8)
	205						

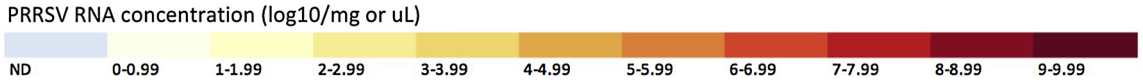

Fig. 3. Fetal preservation status by position and days post inoculation. A) The fetal preservation status of individual fetuses is shown by their relative position in the right (R) or left (L) uterine horn. Fetal meconium staining of face and/or body and death/decomposition increased progressively from 8 days post-inoculation (DPI). B) Mean (SD) PRRSV RNA concentration by tissue and fetal preservation score. Fetal preservation scores: V = viable, F = meconium staining restricted to the face, B = meconium staining on face and body, DEC = decomposed/dead fetus. END = endometrium, PLC = placenta, UMB = umbilical cord, SER = fetal serum, THY = fetal thymus, AMN = amniotic fluid.

19/36 (53%) fetuses. These fetuses, along with two DEC, had high VL in all fetal tissues.

The fetuses in one inoculated gilt (G179) appeared to be largely resistant to PRRSV infection. In spite of high VL in all END samples, no virus was detected in UMB, SER, THY or AMN of any fetus. PRRSV RNA in PLC was not detected in seven and was ultralow (DNQ) in four of the eleven fetuses in this litter. However, meconium staining was observed on the face of one fetus and on the body of another fetus in this litter.

3.2. Classification of resistant, resilient and susceptible fetuses

3.2.1. Classification of fetal susceptibility by DPI

All fetuses at 2 and 5 DPI were VIA with no or low VL. Although they fell into the bottom left quadrant of the fetal resilience matrix (Fig. 4A and B) it was too early to classify as resistant. By contrast, at 8, 12 and 14 DPI (Fig. 4C–E), a select number of fetuses fell into the resilient (top left), susceptible (top right) or ultra-susceptible (bottom right) quadrants. At 8 DPI, this was mainly due to individual fetuses with high VL, whereas at 12 and 14 DPI high VL and fetal preservation score contributed to their classification. The overall proportion of resistant fetuses decreased with duration of infection; from 86% (37/43) at 8 DPI to 42% (15/36) at 14 DPI (Figs. 4D-F).

3.2.2. Factors associated with susceptibility classification

The random forest approach determined which fetal factor(s): DPI, sex, brain:liver ratio, and VL in fetal SER, PLC, UMB, THY and AMN were the strongest predictors of fetal resilience as initially classified using the 2 × 2 fetal resilience (Fig. 4F). The F1 score (average of precision and recall for resistant, resilient, susceptible and ultra-susceptible categories) in the full model was 0.92 and increased to 0.93 following the stepwise removal of: sex, brain:liver ratio, and VL in END, PLC, AMN, UMB and SER. Viral load in END and PLC were the first factors to be removed from the model indicating these tissues were least important determinants of classification. Viral load in AMN and UMB were correlated with THY and SER and when removed from the model had no impact on prediction accuracy. The most parsimonious (final) model contained only DPI and VL in THY. When THY was replaced by SER or DPI was removed, prediction accuracy decreased indicating DPI and THY are the most important predictors of fetal resistance and resilience in this study; however, susceptibility and ultra-susceptibility were poorly predicted by these two factors (Fig. 5A). The precision score (0.97) of the final model exceeded the recall score (0.92) indicating the model had higher specificity and was biased towards producing false negative results (misclassifying true positives) (Fig. 5B). This was most evident with the susceptible group where the final model misclassified 3/5 susceptible fetuses as resilient, and misclassified both ultra-susceptible fetuses. Thus, additional variables or factors are required to better characterize susceptibility. Of the features remaining in the final model, high VL in fetal thymus, non-detectable VL in fetal thymus, and DPI = 14 were the more influential as indicated by their high feature relative importance scores (Fig. 5C).

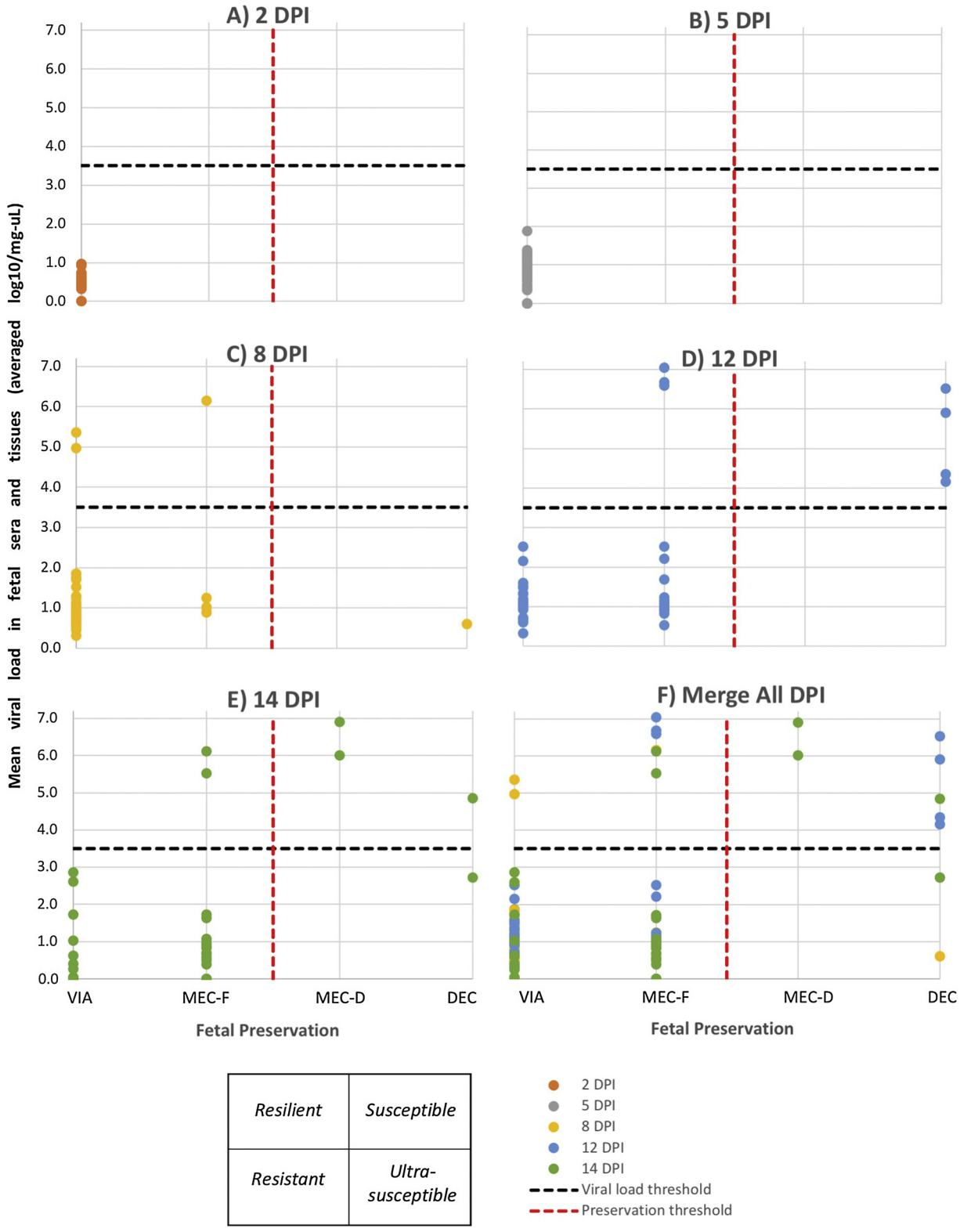

Fig. 4. Susceptible, resistant and resilient fetal matrix. Plots showing relative susceptibility of fetuses to PRRS virus based on mean RNA PRRSV concentration in fetal sera and tissues (placenta, umbilical cord, thymus, amniotic fluid) plotted on Y axis against fetal preservation category (VIA = viable, MEC-F = meconium staining restricted to face, MEC-B = meconium staining on face and body, DEC = decomposed) on X axis. Resistant, resilient, susceptible and ultra-susceptible fetuses are positioned in the bottom-left, top-left, top-right, and bottom-right quadrants, respectively. Dashed lines represent break point thresholds for fetal preservation score (vertical/red) and mean fetal PRRSV RNA concentration (horizontal/black). From 8 DPI onwards, select fetuses are found in the resilience, susceptible and ultra-susceptible quadrants due to changes in their viral load and/or fetal preservation score. DPI = days post inoculation.

A) Classification table

Predicted values \ True values	RT	S	RL	US
RT	53			1
S		2		1
RL		3	2	
US				0
	53	5	2	2

B) Model performance summary

Precision	Recall	F1-score	Support
1.00	0.98	0.99	54
0.40	0.67	0.50	3
1.00	0.40	0.57	5
0.0	1.00	0.0	0
0.97	**0.92**	**0.93**	**62**

C) Relative feature importance

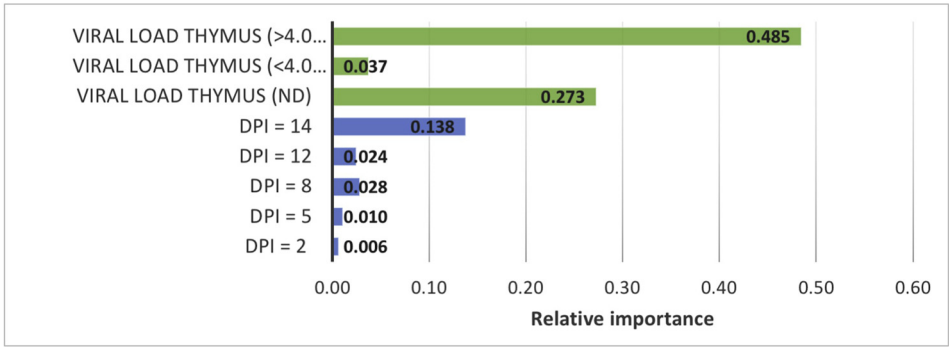

Fig. 5. Classification of resistant, resilient, susceptible fetuses using a random forest model. A forest of 100 trees was created and 205 fetuses from PRRSV inoculated litters were classified using a 70:30 split between training and test datasets. A) Classification matrix of true versus predicted fetuses for each of four susceptibility categories (RT = resistant, S = susceptible, RL = resilient, US = ultra-susceptible). The model was most effective at classifying resistant and resilient fetuses (yellow boxes along diagonal), but misclassified most susceptible and ultra-susceptible fetuses (dark grey boxes). B) Model performance summary: 'precision' (specificity), 'recall' (sensitivity) and 'F1-score' (average of recall and precision) indicate the overall accuracy of 0.93 for the random forest model. 'Support' represents the number of predicted fetuses in each category. C) After developing the full model, a backwards stepwise removal of least important variables (pruning) was performed to create a parsimonious model. The relative importance of variables (features) left in the model is shown and indicates that thymic viral load > 4 $\log_{10}$/mg or not detected (negative) and 14 days post inoculation (DPI) were the most important features required for classification. By contrast, fetal sex, brain:liver ratio (IUGR), and viral load in endometrium, placenta, fetal sera, amniotic fluid and umbilic cord were not important predictors of fetal susceptibility, resilience or resistance in this study.

3.3. Relationship of IUGR to VL and fetal preservation

The brain: liver ratio averaged 1.34 (± 0.34; SD) across all fetuses and was significantly greater in fetuses of non-inoculated versus inoculated gilts (CTRL = 1.44 ± 0.35; INOC = 1.31 ± 0.33; P = 0.006). Because the brain: liver ratio changes in accordance with fetal growth, the mean brain: liver ratio was calculated for each DPI (only INOC gilts): 2 DPI = 1.15 (± 0.22), 5 DPI = 1.26 (± 0.29), 8 DPI = 1.54 (± 0.24), 12 DPI = 1.37 (± 0.33), and 14 DPI = 1.36 (± 0.44). Using plus or minus 1 SD as breakpoints to identify IUGR and non-IUGR fetuses, respectively, 21/203 (10.8%) fetuses were classified as non-IUGR, 155/203 (76.4%) as average (AVG), and 27/203 (13.3%) as IUGR in PRRSV inoculated litters (2 fetuses did not have their brain or liver weighed). There was a trend towards more non-IUGR fetuses being compromised (MEC or DEC) compared to AVG and IUGR fetuses when all five DPI were combined (P = 0.06), but this was largely the result of group differences observed at 12 DPI. Non-IUGR fetuses had significantly higher VL in UMB, SER and AMN than IUGR or AVG fetuses at 14 DPI, and in THY across all days. There were no differences of VL in END and PLC amongst the three groups (Fig. 6).

4. Discussion

This study investigated the rate of PRRSV transmission across the maternal-fetal interface and the development of fetal compromise at five different time points post inoculation. Although our research group has undertaken a number of PRRSV-2 pregnant gilt challenge experiments in the past, the results reported herein are novel in terms of investigating maternofetal transmission across range of termination days, assessment of viral load across multiple fetal tissues and elucidation of the pathogenesis and potential factors associated with fetal PRRSV resistance/resilience. In spite of the small number of fetuses spread over five termination time points (14 post inoculation days), several important conclusions can be drawn from the study.

The rapidity at which the END and PLC were infected cannot be under-emphasized and has implications for investigating potential routes of transplacental transmission of the virus. Nearly all END and PLC samples were infected at 2 DPI. Early endometrial infection was expected, as infected gilts are viremic at 1 DPI (Zimmerman et al., 2012), but the rapid infection of PLC indicates that the mechanism of transplacental infection is likely efficient and initiates concurrently with viremia. While macrophage-associated transmission of virus from END to PLC has been proposed (Karniychuk and Nauwynck, 2013), PRRSV may use several routes to transmit into fetuses. The interdigitations of the dual epithelial layers of the porcine MFI prevents the transmission of large macromolecules, but allows for the efficient exchange of nutrients and gasses across short diffusion distances (Bazer and Johnson, 2014). Inflammation, apoptosis or necrosis of maternal uterine epithelium and fetal trophoblast may alter cell membrane and tight junction integrity allowing direct transmission within or between cells. However, even before epithelial cell integrity is affected, extracellular vesicles may provide an efficient, rapid mechanism of viral transmission across the MFI. Extracellular vesicles are important carriers of lipids, proteins and nucleic acids and play a vital role in fetal-maternal communication in humans (Cronqvist et al., 2017; Tong and Chamley, 2015) and pigs (Bidarimath et al., 2017). Bidirectional shuttling of extracellular vesicles containing miRNAs between fetal trophoblast and maternal endothelial cells has been demonstrated *in vitro* and may be a "trojan horse" method of transmission. Exosomes have been implicated in the transmission of PRRSV, having been shown to contain viral genomic RNA and partial viral proteins, and establish productive infections in PK-15 and Marc-145 cells in vitro (Wang et al., 2018).

It is important to note that steps were taken to prevent the cross-contamination of placenta with maternal blood during sample collection, to reduce the likelihood of false positive PCR results of PLC.

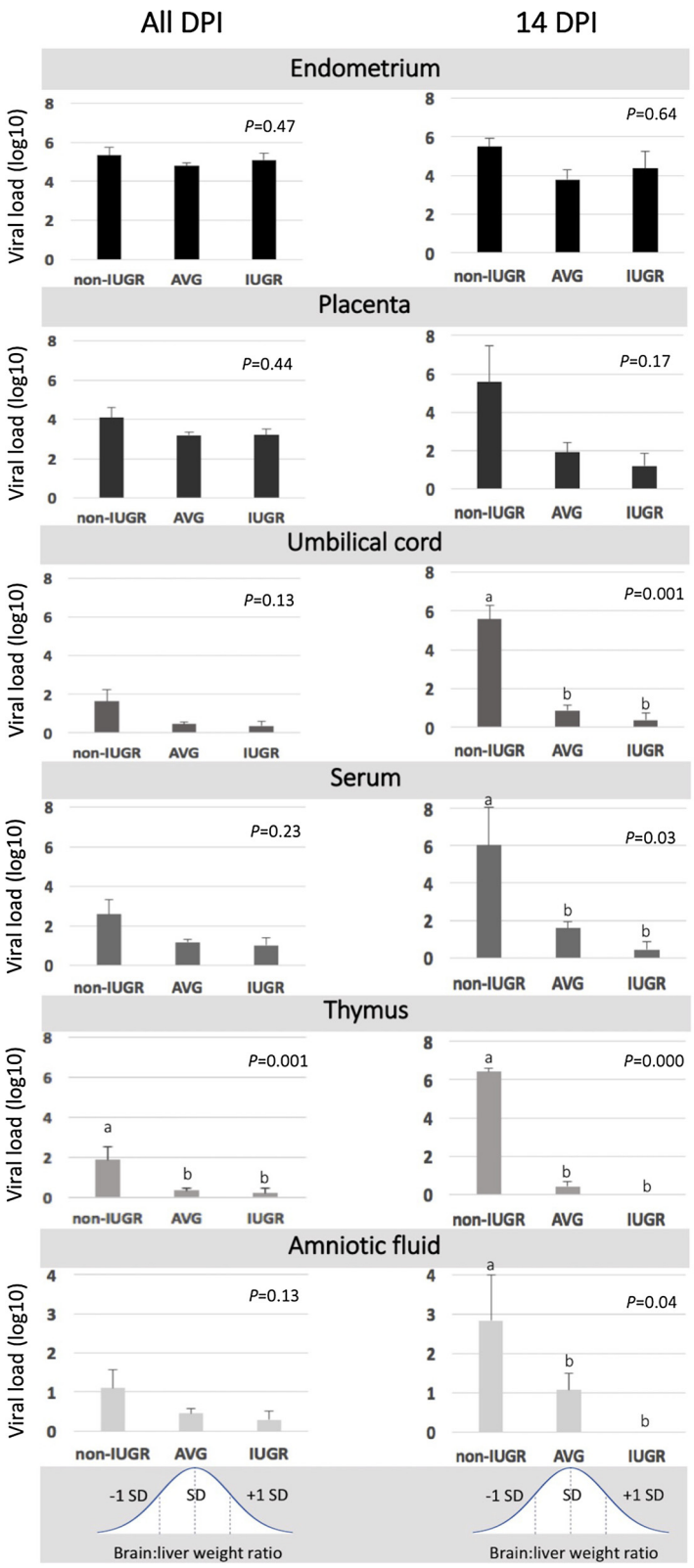

Fig. 6. PRRSV RNA concentration (viral load) by IUGR group in fetal tissues and sera. Bar plots show the difference in viral load in endometrium, placenta, umbilical cord, fetal serum, thymus and amniotic fluid averaged across all days post inoculation (DPI; left) and at 14 DPI (right). The belt shape curves beneath the bar plots indicate how the three IUGR groups were defined: IUGR = < -1 SD below mean, non-IUGR = > 1 SD above mean, AVG = between -1 and +1 SD from the mean. Compared to IUGR and average fetuses, viral load in non-IUGR fetuses was significantly greater in THY across all DPI, and in umbilical cord, serum and amniotic fluid at 14 DPI.

However, separating the placenta from endometrium is a delicate process, and when poorly performed can result in small amounts of endometrium adhering to the placental portion of the sample (unpublished data). To minimize the risk of contaminating the placental samples, this task was limited to a small team of experienced and proficient technicians. Furthermore, viral presence was assessed in a subset of fetuses across all DPI using immunofluorescent analyses that confirmed the presence of PRRSV antigen in placental tissue on 2 DPI (Suleman et al., 2018). Moreover, there was a moderate correlation between PRRSV RNA concentration (assessed using RT-qPCR) and viral antigen spot counts (assessed using immunofluorescence) in END and PLC (Suleman et al., 2018).

After placental infection, the virus presumably replicates in permissive placental macrophages until it enters the fetal circulation. We

observed the first evidence of viral RNA in UMB and fetal sera at 5 DPI. The positivity of the umbilical cord indicates PRRSV migrates from the placenta to the fetus through the umbilical blood circulation. In spite of that, we observed detection of virus in AMN within some fetuses, but not in their UMB or SER, suggesting the possibility of horizontal viral transmission through the placental membranes instead of the umbilical cord circulation. A previous study indicated that PRRSV may be transmitted from fetus to fetus via sibling microchimeric cells, crossing in between adjacent extremities of the fetal allantochorion (Karniychuk et al., 2012).

Thymus is the putative primary fetal site for virus replication (Rowland, 2010). Our results clearly show that PLC is the initial fetal tissue for PRRSV replication, as it was infected within 2 days of inoculation, reaching high VL prior to any other fetal tissue. The first positive THY and AMN samples were detected at 8 DPI, demonstrating that the virus replicates in other fetal locations at first. However, THY may become the main fetal site of viral replication after about one week of infection, as it reached high VL quickly. The high PRRSV RNA concentration in THY when first detected indicates that the virus was possibly replicating there prior to 8 DPI. Unfortunately, we did not quantify PRRSV RNA concentration in THY or other systemic fetal sites between 5 and 8 DPI.

The first signs of fetal compromise were observed at 8 DPI, implying that the virus requires about one week of infection and replication to initiate whatever cascade of events jeopardizes fetal health and survival. Unexpectedly, the first observed DEC fetus was RT-qPCR negative in all fetal tissues and had no evidence of vasculitis and placental detachment, and only minimal placentitis based on assessments reported by Novakovic et al. (2018). While the mechanism of fetal death is complex and poorly understood, this fetus is clearly an outlier and may have died for a reason unrelated to PRRSV infection. The number of MEC and DEC fetuses steadily increased after 8 DPI, and more severe meconium staining of face and body was generally associated with higher PRRSV RNA concentration. Categorizing meconium staining based on location (face or face and body) was useful in this study to demonstrate the progression of disease over time. We believe that fetuses with deposits of meconium on their faces and bodies would likely die within a few days if pregnancy was continued without interruption. A previous study in which PRRSV infected pregnant gilts were euthanized at 21 DPI had more than 40% dead fetuses (Ladinig et al., 2014b) compared to only 8% and 5% at 12 and 14 DPI, respectively in this study, emphasizing how rapidly the maternofetal environment decays.

Fetal resistance, resilience and susceptibility have not been formally defined in the context of PRRSV infection but may help lead to new control strategies if mechanisms of resistance are understood. In the present study, susceptible fetuses were easily identified as non-viable (MEC or DEC) with high VL in multiple fetal tissues. Resistant and resilient fetuses were harder to identify. Viable fetuses with high VL across multiple tissues were considered resilient, defined as the ability of the animal to not become compromised despite high infections (Richardson, 2016) or sustained performance in the face of infection (Bishop and Woolliams, 2014). By contrast, resistance implies an animal's ability to exert control over the pathogen's life cycle, or replication in the case of PRRSV (Bishop and Woolliams, 2014). Resistance is typically relative rather than absolute, as observed in the present study. Resistant fetuses were VIA with negative or low VL in the majority of tissues. This is clearly an ideal characteristic to achieve and based on the results of this study, appear to occur at the fetal or gilt level. For example, the litter of G179 was almost completely RT-qPCR negative at 14 DPI. While high VL and the presence of fetal lesions are definitive risk factors for meconium staining (Ladinig et al., 2015a; Novakovic et al., 2018), it was not a factor in these fetuses. It is possible that these fetuses were responding to physiologic changes related to the infection of PLC and/or END, as has been previously elucidated (Wilkinson et al., 2016). As resistance does not need to be complete (Bishop and Woolliams, 2014), achieving partial resistance (reduction in VL or a proportion of negative animals, or both) might be a more achievable goal in the swine industry. However, we acknowledge that because animals were terminated earlier in this study than many reproductive PRRS studies and natural swine pregnancy (115 days), it is difficult to predict how many of the fetuses classified as resistant or resilient would have died if the pregnancy continued to term.

Using fetal VL and fetal preservation status as an initial classification system allowed visualization of susceptible, resistant and resilient fetuses in a 2×2 matrix. While the fetuses occupied multiple quadrants at 8 and 12 DPI, the random forest classification model strongly indicated that 14 DPI was a more important feature for accurate classification than earlier DPI ($< = 12$). Moreover, VL in THY was a more important classifier than VL in SER or other fetal tissues. It must be noted that the random forest analysis was undertaken herein on a very small dataset with a limited number of variables, some highly correlated. While showing proof of concept in classifying fetal susceptibility, resistance and resilience, it is necessary to perform similar analyses on larger and more complex datasets to improve confidence in these findings. Although sparsely used in veterinary epidemiology, random forest models have been used with success to study relevant swine industry health-related problems such as swine influenza, salmonellosis, and biosecurity effectiveness (Abrahantes et al., 2009; Holtkamp et al., 2012; Hu, 2010; Larison et al., 2014; Valdes-Donoso et al., 2017; White et al., 2017).

A previous study unexpectedly showed that non-IUGR ("larger") fetuses have higher VL compared to fetuses experiencing IUGR (Ladinig et al., 2014a). Here, we confirmed that non-IUGR fetuses have higher VL in all the fetal tissues at 14 DPI, but not in END and PLC, indicating that the consequences of IUGR only affect the fetus. The absence of IUGR group differences before 14 DPI is likely because insufficient time had elapsed for transplacental infection and viral replication in the fetal tissues. IUGR is a condition where individual fetuses are deprived of nutrients and, thus, have a restricted growth in the uterus. There are many factors that can lead to this condition, such as genetics, endocrine and environmental disruption. When it occurs, it favors brain development at the expense of other organs (Fowden and Forhead, 2004). It was demonstrated that IUGR fetuses have altered placental structures, which can lead to alterations in nutrient absorption from the dam (Chen et al., 2015). This concept might be applicable to transplacental PRRSV infection. The fact that IUGR fetuses have smaller PLC might result in fetuses that are less prone to infection. However, determining if any structural or cellular changes occur in IUGR tissues may lead to method (s) to prevent or reduce transmission to non-IUGR animals.

5. Conclusions

This was the first temporal study assessing PRRSV RNA concentration in fetal tissues at five different time points over 14 days post-inoculation to investigate the progression of PRRSV infection and disease. Our results confirmed that the maternal-fetal interface (END, PLC) is promptly infected at 2 DPI after maternal inoculation and that PRRSV replicates in PLC before entering the fetal circulation on 5 DPI. Fetal compromise was first observed on 8 DPI and increased progressively through 14 DPI. Although samples were not assessed each day between 2 and 14 DPI, we affirm that the virus takes around a week to sufficiently replicate in fetal tissues to induce fetal compromise. Variation in fetal resistance, resilience and susceptibility, most strongly associated with VL in fetal THY compared to other fetal tissues, was first evident beginning at 8 DPI, but was more clearly discernable at later DPI. Viral load in fetal tissues was greater in non-IUGR fetuses, confirming previous research, but brain: liver ratio was not a predictor of fetal resilience, resistance or susceptibility. Collectively, these findings shed new light on the mechanics of fetal PRRSV infection and resilience.

Ethics approval

This study was approved by the University of Saskatchewan Animal Research Ethics Board and adhered to the Canadian Council on Animal Care guidelines for humane animal use (protocol #2016002). The infected pregnant gilts were closely monitored for clinical signs and a human intervention point checklist was established to monitor the gilts for critical conditions post-inoculation. It was not feasible to monitor fetal conditions after the viral inoculation, but fetal compromise death was expected to occur at the later time points. We selected termination points that were prior to when a high rate of fetal death was expected. Gilts were euthanized with intravenous sodium pentobarbital overdose followed by pithing and exsanguination. Fetuses were euthanized as humanely as possible given that pentobarbital sodium crosses the MFI rapidly (Fishman and Yanai, 1983; RXmed, 2018) and enters fetal circulation prior to the onset of hypoxia and asphyxia.

Availability of data and material

Data will be made available to researchers with a legitimate hypothesis and objectives. Please contact the corresponding author.

Competing interests

The authors declare no conflicts of interest with respect to the research, authorship and/or publication of this article.

Funding

This project was supported by Genome Canada (grant #345169) and Genome Prairie (Saskatchewan Ministry of Agriculture; grant #20150329), along with administrative support provided by Genome Alberta and the University of Saskatchewan. The funding agencies had no involvement in study design, implementation, analyses or interpretation of the results.

Authors' contributions

CM: sample collection, tissue viral RNA extraction, RT-qPCR analysis, statistical analysis, manuscript preparation; RN: sample collection, RNA extraction, RT-qPCR; LR: sample collection; PN, MS, AL, SD, DM, JH: experimental design, sample collection; JH: project and financial management, statistical analysis, manuscript preparation.

Acknowledgements

We express special acknowledgment to numerous personnel (technicians, graduate students, summer students, colleagues) who helped in the preparation and implementation of this study. Animal Care was contracted to VIDO-Intervac, Saskatoon. Necropsies were performed at the Prairie Diagnostic Services, Saskatoon.

Appendix A. Supplementary data

Supplementary material related to this article can be found, in the online version, at doi:https://doi.org/10.1016/j.virusres.2018.12.002.

References

Cortinas Abrahantes, J., Bollaerts, K., Aerts, M., Ogunsanya, V., Stede, Yvd., 2009. Salmonella serosurveillance: different statistical methods to categorise pig herds based on serological data. Prev. Vet. Med. 89 (1/2), 59–66.

Bazer, F.W., Johnson, G.A., 2014. Pig blastocyst-uterine interactions. Differentiation 87 (1-2), 52–65.

Bidarimath, M., Khalaj, K., Kridli, R.T., Kan, F.W.K., Koti, M., Tayade, C., 2017. Extracellular vesicle mediated intercellular communication at the porcine maternal-fetal interface: a new paradigm for conceptus-endometrial cross-talk. Sci. Rep. 7, 40476.

Bishop, S.C., Woolliams, J.A., 2014. Genomics and disease resistance studies in livestock. Livest. Sci. 166, 190–198.

Chen, F., Wang, T., Feng, C., Lin, G., Zhu, Y., Wu, G., Johnson, G., Wang, J., 2015. Proteome differences in placenta and endometrium between normal and intrauterine growth restricted pig fetuses. PLoS One 10 (11), e0142396.

Cronqvist, T., Tannetta, D., Mörgelin, M., Belting, M., Sargent, I., Familari, M., Hansson, S.R., 2017. Syncytiotrophoblast derived extracellular vesicles transfer functional placental miRNAs to primary human endothelial cells. Sci. Rep. 7, 4558.

Fishman, R.H.B., Yanai, J., 1983. Long-lasting effects of early barbiturates on central nervous system and behavior. Neurosci. Biobehav. Rev. 7 (1), 19–28.

Fowden, A.L., Forhead, A.J., 2004. Endocrine mechanisms of intrauterine programming. Reproduction 127 (5), 515–526.

Ge, M., Zhang, Y., Liu, Y., Liu, T., Zeng, F., 2016. Propagation of field highly pathogenic porcine reproductive and respiratory syndrome virus in MARC-145 cells is promoted by cell apoptosis. Virus Res. 213, 322–331.

Holtkamp, D.J., Lin, H., Wang, C., O'Connor, A.M., 2012. Identifying questions in the American Association of Swine Veterinarian's PRRS risk assessment survey that are important for retrospectively classifying swine herds according to whether they reported clinical PRRS outbreaks in the previous 3 years. Prev. Vet. Med. 106 (1), 42–52.

Holtkamp, D., Kliebenstein, J., Neumann, E., Zimmerman, J., Rotto, H., Yoder, T., Wang, C., Yeske, P., Mowrer, C., Haley, C., 2013. Assessment of the economic impact of porcine reproductive and respiratory syndrome virus on United States pork producers. J. Swine Health Prod. 21 (2), 72–84.

Hu, W., 2010. Nucleotide host markers in the influenza A viruses. J. Biomed. Sci. Eng. 3 (7), 684–699.

Karniychuk, U.U., Nauwynck, H.J., 2009. Quantitative changes of sialoadhesin and CD163 positive macrophages in the implantation sites and organs of porcine embryos/fetuses during gestation. Placenta 30 (6), 497–500.

Karniychuk, U.U., Nauwynck, H.J., 2013. Pathogenesis and prevention of placental and transplacental porcine reproductive and respiratory syndrome virus infection. Vet. Res. 44, 95.

Karniychuk, U.U., Van Breedam, W., Van Roy, N., Rogel-Gaillard, C., Nauwynck, H.J., 2012. Demonstration of microchimerism in pregnant sows and effects of congenital PRRSV infection. Vet. Res. 43, 19.

Karniychuk, U.U., De Spiegelaere, W., Nauwynck, H.J., 2013. Porcine reproductive and respiratory syndrome virus infection is associated with an increased number of Sn-positive and CD8-positive cells in the maternal-fetal interface. Virus Res. 176 (1-2), 285–291.

Ladinig, A., Foxcroft, G., Ashley, C., Lunney, J.K., Plastow, G., Harding, J.C.S., 2014a. Birth weight, intrauterine growth retardation and fetal susceptibility to porcine reproductive and respiratory syndrome virus. PLoS One 9 (10), e109541.

Ladinig, A., Wilkinson, J., Ashley, C., Detmer, S.E., Lunney, J.K., Plastow, G., Harding, J.C.S., 2014b. Variation in fetal outcome, viral load and ORF5 sequence mutations in a large scale study of phenotypic responses to late gestation exposure to type 2 porcine reproductive and respiratory syndrome virus. PLoS One 9 (4), e96104.

Ladinig, A., Ashley, C., Detmer, S.E., Wilkinson, J.M., Lunney, J.K., Plastow, G., Harding, J.C.S., 2015a. Maternal and fetal predictors of fetal viral load and death in third trimester, type 2 porcine reproductive and respiratory syndrome virus infected pregnant gilts. Vet. Res. 46, 107.

Ladinig, A., Detmer, S.E., Clarke, K., Ashley, C., Rowland, R.R., Lunney, J.K., Harding, J.C., 2015b. Pathogenicity of three type 2 porcine reproductive and respiratory syndrome virus strains in experimentally inoculated pregnant gilts. Virus Res. 203, 24–35.

Lager, K., Mengeling, W., 1995. Pathogenesis of in utero infection in porcine fetuses with porcine reproductive and respiratory syndrome virus. Can. J. Vet. Res. 59 (3), 187–192.

Larison, B., Njabo, K.Y., Chasar, A., Fuller, T., Harrigan, R.J., Smith, T.B., 2014. Spillover of pH1N1 to swine in Cameroon: an investigation of risk factors. BMC Vet. Res. 10 (55) 4 March 2014.

Machado, G., Mendoza, M.R., Corbellini, L.G., 2015. What variables are important in predicting bovine viral diarrhea virus? A random forest approach. Vet. Res. 46 (1), 85.

Novakovic, P., Harding, J.C., Al-Dissi, A.N., Ladinig, A., Detmer, S.E., 2016. Pathologic evaluation of type 2 porcine reproductive and respiratory syndrome virus Infection at the maternal-fetal interface of late gestation pregnant gilts. PLoS One 11 (3), e0151198.

Novakovic, P., Harding, J.C., Al-Dissi, A.N., Detmer, S.E., 2017. Type 2 porcine reproductive and respiratory syndrome virus infection increases apoptosis at the maternal-fetal interface in late gestation pregnant gilts. PLoS One 12 (3), e0173360.

Novakovic, P., Detmer, S.E., Suleman, M., Malgarin, C.M., MacPhee, D.J., Harding, J.C.S., 2018. Histologic changes associated with placental separation in gilts infected with porcine reproductive and respiratory syndrome virus. Vet. Pathol. 55 (4), 521–530.

Richardson, L.A., 2016. Understanding disease tolerance and resilience. PLoS Biol. 14 (7), e1002513.

Rowland, R.R., 2010. The interaction between PRRSV and the late gestation pig fetus. Virus Res. 154 (1-2), 114–122.

RXmed, 2018. Barbiturates (Amobarbital). (Accessed 28 September 2018). https://www.rxmed.com/b.main/b2.pharmaceutical/b2.1.monographs/cps-_monographs/CPS-_(General_Monographs-_B)/BARBITURATES.html.

Suleman, M., Galea, S., Gavard, F., Merillon, N., Klonjkowski, B., Tartour, E., Richardson, J., 2011. Antigen encoded by vaccine vectors derived from human adenovirus serotype 5 is preferentially presented to CD8+ T lymphocytes by the CD8alpha+ dendritic cell subset. Vaccine 29 (35), 5892–5903.

Suleman, M., Novakovic, P., Malgarin, C.M., Detmer, S.E., Harding, J.C.S., MacPhee, D.J.,

2018. Spatiotemporal immunofluorescent evaluation of porcine reproductive and respiratory syndrome virus transmission across the maternal-fetal interface. Pathog. Dis fty060-fty060.
Terpstra, C., Wensvoort, G., Pol, J.M., 1991. Experimental reproduction of porcine epidemic abortion and respiratory syndrome (mystery swine disease) by infection with Lelystad virus: Koch's postulates fulfilled. Vet. Q. 13 (3), 131–136.
Tong, M., Chamley, L.W., 2015. Placental extracellular vesicles and feto-maternal communication. Cold Spring Harb. Perspect. Med. 5 (3), a023028.
Valdes-Donoso, P., VanderWaal, K., Jarvis, L.S., Wayne, S.R., Perez, A.M., 2017. Using machine learning to predict swine movements within a regional program to improve control of infectious diseases in the US. Front. Vet. Sci. 4 (January), 2.
Van Gorp, H., Van Breedam, W., Delputte, P.L., Nauwynck, H.J., 2008. Sialoadhesin and CD163 join forces during entry of the porcine reproductive and respiratory syndrome virus. J. Gen. Virol. 89 (Pt 12), 2943–2953.
Wang, T., Fang, L., Zhao, F., Wang, D., Xiao, S., 2018. Exosomes mediate intercellular transmission of porcine reproductive and respiratory syndrome virus. J. Virol. 92 (4).
White, L.A., Torremorell, M., Craft, M.E., 2017. Influenza A virus in swine breeding herds: combination of vaccination and biosecurity practices can reduce likelihood of endemic piglet reservoir. Prev. Vet. Med. 138, 55–69.
Whitworth, K.M., Prather, R.S., 2017. Gene editing as applied to prevention of reproductive porcine reproductive and respiratory syndrome. Mol. Reprod. Dev. 84 (9), 926–933.
Wilkinson, J.M., Bao, H., Ladinig, A., Hong, L., Stothard, P., Lunney, J.K., Plastow, G.S., Harding, J.C.S., 2016. Genome-wide analysis of the transcriptional response to porcine reproductive and respiratory syndrome virus infection at the maternal/fetal interface and in the fetus. BMC Genomics 17 (1), 1–17.
Zimmerman, J.J., Benfield, D.A., Dee, S.A., Murtaugh, M.P., Stadejek, T., Stevenson, G.W., Torremorell, M., 2012. Porcine reproductive and respiratory syndrome virus (Porcine Arterivirus). In: Zimmerman, J.J., Karriker, L., Ramirez, A., Schwartz, K.J., Stevenson, G.W. (Eds.), Diseases of Swine, 10th edition. Wiley-Blackwell, Ames, IA, pp. 461–486.